Amino Acids (2014) 46:1839–1851
DOI 10.1007/s00726-014-1698-y

ORIGINAL ARTICLE

Deciphering aggregates, prefibrillar oligomers and protofibrils of cytochrome c

Samreen Amani · Aabgeena Naeem

Received: 5 June 2013 / Accepted: 14 February 2014 / Published online: 12 April 2014

Abstract Aggregation of protein into insoluble intracellular complexes and inclusion bodies underlies the pathogenesis of human neurodegenerative diseases. Importance of cytochrome c (cyt c) arises from its involvement in apoptosis, sequence homology and for studying molecular evolution. A systemic investigation of polyethylene glycol (PEG) and trifluoroethanol (TFE) on the conformational stability of cyt c as a model hemeprotein was made using multi-methodological approach. Cyt c exists as molten globule (MG) at 60 % PEG-400 and 40 % TFE as confirmed by far-UV CD, attenuated total reflection Fourier transform infrared spectroscopy, Trp environment, 8-anilino-1-naphthalene-sulfonic acid (ANS) binding and blue shift in the soret band. Q-band splitting in MG states specifies conformational changes in the hydrophobic heme-binding pocket. Aggregates were detected at 90 % PEG-400 and 50 % TFE as confirmed by increase thioflavin T and ANS fluorescence and shift in Congo red absorbance. Detection of prefibrils and protofibrils at 90 % PEG-400 and 50 % TFE was possible after 72-h incubation. Single cell gel electrophoresis of prefibrils and protofibrils showed DNA damage confirming their toxicity and potential health hazards. Scanning electron microscopy and XRD analysis confirmed prefibrillar oligomers and protofibrils of cyt c.

Keywords Cytotoxicity · Partially folded intermediate · Partially unfolded intermediate · Polyethylene glycol · Trifluoroethanol

S. Amani · A. Naeem (✉)
Department of Biochemistry, Faculty of Life Science, Aligarh Muslim University, Aligarh 202002, India
e-mail: abgeenanaim@rediffmail.com; aabgeenanaim@gmail.com; anaeem.bc@amu.ac.in

S. Amani
e-mail: samreen.amani@gmail.com

Introduction

Protein misfolding and aggregation is a topic of great interest due to its significance in biotechnology and the occurrence of protein deposits in a variety of diseases. These diseases include the amyloidosis, the most prominent neurodegenerative diseases like Alzheimer's and Parkinson's disease and the prion diseases. Protein deposits linked with diseases are characterized by high cross β-sheet content and are referred to as amyloid or amyloid-like if they show fibrillar morphology. During the final stages of systemic amyloidosis, amyloid plaques lead to dysfunction and organ rupture. Whether the mechanism of protein aggregation and deposition is an epiphenomenon or a cause of neurodegenerative diseases is a matter of debate, apart from the prion diseases where overwhelming experimental evidence suggests that protein deposits or their precursors are the infectious agents responsible for transmission of disease (Kraus et al. 2013; Naeem and Fazili 2011; Wood et al. 2003). Protein aggregation arises as a result of misfolding in response to mutations, posttranslational modification or changes in local conditions such as pH and temperature. Aggregates are produced when folded or unfolded intermediates interact mainly through contact of their hydrophobic surfaces, turning into large, stable complexes (Amani and Naeem 2013a; Turnell and Finch 1992).

Destabilization caused by addition of organic solvent is one of the most employed strategies used for structural alteration resulting in protein aggregation. Polyethylene glycol (PEG) is a drug used as an excipient in pharmaceutical products, as an osmotic laxative for bowel preparation and in cosmetics. It causes slow release of proteins when attached to protein medications and is also used to treat chronic or intermittent constipation. The diacid

metabolites of low-molecular-weight PEGs are excellent calcium chelators and can account for the hypercalcemia. PEG metabolites also cause renal destruction (Herold et al. 1982). 2,2,2-Trifluoroethanol (TFE) and its derivatives are commonly used as inhalation anesthetics. It is also used industrially as a solvent for nylon, as a dye and as an ingredient in anti-ulcer agents, anti-arrhythmic drugs etc. Toxicity of TFE has been confirmed on blood, male reproductive system, brain, upper respiratory tract and eyes (Zerovnik et al. 2007). It shifts the equilibrium from native toward denatured state and thus favoring aggregation and subsequent fibril formation. TFE also impersonate the role of membranes in inducing structural alterations and aggregation of protein, which make this type of study commendable for analyzing protein conformation.

Cytochrome c (cyt c) is a highly conserved (~12 kDa) protein consisting of 104 amino acid hemeprotein whose principal biological function is electron transport and apoptosis. It consists of a single heme group, which is covalently attached to Cys14 and Cys17. Because of its ubiquitous nature and sequence homology, cyt c has been used as a model protein for molecular evolution (Margoliash 1963). It is known to be involved in a number of diseases including Alzheimer's and Parkinson's where its over-expression cause apoptosis of vital cells and hence disease (Fiskum et al. 2003). TFE is a very well-known agent which induces β-sheet to α-helix transition in various proteins. It also stabilizes partially folded states of proteins and can be used as promoter of amyloid formation (e.g., in different proteins including α-chymotrypsin). Thus, in the present study, PEG-400 and TFE are chosen for inducing conformational changes in cyt c. In the present work, we explore aspects of the formation of aggregates, prefibrils and protofibrils of cyt c by a combination of CD, FTIR and EM to gain insight into the events underlying the structural transformation of a highly helical protein to largely β-sheet amyloid fibrils. This study will also provide information that might help to understand the molecular basis of amyloid diseases and a better understanding of the aggregation properties which is an essential step for developing diagnostic tests and therapeutic strategies.

Materials and methods

Cyt c, TFE, PEG-400, 8-anilino-1-naphthalene-sulfonic acid (ANS), thioflavin T (ThT) and Congo red (CR) were procured from Sigma (St. Louis, MO, USA); Sodium phosphate monobasic and dibasic was also purchased from Sigma (St. Louis, MO, USA) for making sodium phosphate buffer of pH 7.

Stock solution of cyt c (5 mg/ml) was prepared in 20 mM sodium phosphate buffer, pH 7, and it was then dialyzed in the same buffer. The concentration of native protein in 20 mM sodium phosphate buffer, pH 7, was determined from extinction coefficient of 10.6×10^4 M/cm by UV absorption at 410 nm on a Shimadzu UV-1700 spectrometer.

Effect of PEG-400 and TFE on cyt c

Aliquots of cyt c were prepared with varying concentration of PEG from 0 to 90 % v/v and for TFE from 0 to 50 % v/v (Unless otherwise indicated all the concentration are present in percentage v/v). Aliquots were incubated for 4 h at 27 °C prior to performing spectroscopic measurements. Three replicates for each set were analyzed for the results. Spectral subtraction has been performed with the help of software available in Shimadzu RF-5301 spectrofluorophotometer. This software records the reading of blank aliquot of solvents in the absences of protein. Later signals of aliquot having solvent and protein were recorded. Then, both these signals were subtracted, and final subtracted spectra are presented by the software.

Trp fluorescence measurements

The fluorescence spectra were recorded on a Shimadzu RF-5301 spectrofluorophotometer (Tokyo, Japan) in a 1-cm path length quartz cell. The excitation wavelength was 295 nm, and the emission was recorded in the range of 300–400 nm (Stryer 1968). Final concentration of protein in each aliquot was 16.66 μM.

Acrylamide-quenching study

In the acrylamide-quenching experiments, to achieve the desired acrylamide concentration, aliquots of 5 M acrylamide stock solution were added to a protein stock solution (15 μM). Excitation wavelength was set at 295 nm to excite Trp fluorescence only, and the emission spectrum was recorded in the range 300–400 nm. Decrease in fluorescence intensity at λ_{max} was analyzed according to the Stern–Volmer equation (Eftink and Ghiron 1982):

$$\frac{F_0}{F} = 1 + K_{sv}[Q]$$

where F_0 and F are the fluorescence intensities at an appropriate wavelength in the absence and presence of a quencher (acrylamide), respectively; K_{sv} is the Stern–Volmer constant for the collisional quenching process, and $[Q]$ is the concentration of the quencher.

ANS fluorescence measurements

ANS binding was measured by fluorescence emission spectra with excitation at 380 nm, and emission was recorded from 400 to 600 nm. ANS concentration was 100

molar excess of protein concentration, and protein was 16.66 μM (Stryer 1965).

Soret absorbance spectroscopy

The soret absorption of the heme group was monitored by a Shimadzu UV-1700 spectrophotometer, using a 10-mm path length cell. The final concentration of protein in aliquots was 16.66 μM, and the recording range was 350–710 nm.

Circular dichroism (CD) measurements

Circular dichroism (CD) was measured with a JASCO J-815 spectropolarimeter calibrated with ammonium D-10-camphorsulfonate. Cells of path lengths 0.1 and 1 cm were used for scanning between 250–200 and 300–250 nm, respectively. Each spectrum was the average of 4 scans for good signal-to-noise ratio. Protein concentration for the scans was 16.66 μM for far-UV and 83.3 μM for near-UV spectra. The results were expressed as mean residue ellipticity (MRE) in deg cm^2/dmol which is defined as:

$$\mathrm{MRE} = \frac{\theta_{\mathrm{obs}}(m^{\circ})}{10XnXCpXl}$$

where θ_{obs} is the CD in millidegree, '*n*' the number of residues, *Cp* the molar fraction, that is, concentration/molar mass, and '*l*' the length of light path in centimeters (Naeem and Khan 2004).

Attenuated total reflection Fourier transform infrared spectroscopy (ATR-FTIR)

FTIR spectra were recorded with an Interspec 2020 FTIR spectrometer in deuterated buffer of pH 7. The samples for FTIR studies were prepared by dissolving intermediate and aggregated states of cyt c in deuterated buffer. Solutions are placed between two CaF_2 windows with a spacer. Since the D_2O bend vibration absorbs strongly below 1,500 cm^{-1}, the path length must be kept to a minimum; therefore, sample concentrations must be relatively high. Protein concentration was 140 μM. The scanning wave number was from 1,000 to 4,000 cm^{-1} (Naeem et al. 2011).

Thioflavin T assay

Fluorescence spectra were recorded with a Shimadzu RF-5301 spectrofluorophotometer in a 10-mm path length quartz cell. The excitation wavelength was 440 nm, and the emission was recorded from 450 to 600 nm (Amani and Naeem 2011). For aggregation studies, ThT was added to the aliquots incubated for 4 h, and then, readings were recorded after 24 h. Final concentration of protein in the aliquot was 16.66 μM while ThT was 83.5 μM. ThT was prepared in 20 mM sodium phosphate buffer, pH 7.

Congo red

Absorption spectra were recorded in the range between 400 and 700 nm on Shimadzu UV-1700 spectrophotometer. Aliquots were prepared with protein concentration of 1 mg/ml. Sixty microliters of each aliquot is added to 440 μl of a solution containing 20 μM CR in 20 mM phosphate buffer and thus maintaining a ratio of 1:4 (Eisert et al. 2006). After 2–3 min of equilibration, absorbance was recorded.

Aggregation kinetics

Time-course changes accompanying cyt c misfolding and aggregation were performed by sampling aliquots of a cyt c aggregation reaction at different time points. The fluorescent dyes ANS and ThT were employed in kinetic assays to characterize the oligomeric and protofibrillar states of cyt c using steady-state fluorescence techniques. The aggregation reaction of native cyt c (16.66 μM) was initiated by adding 90 % PEG-400 and 50 % TFE to 20 ml solution of protein in 20 mM phosphate buffer, pH 7. Aliquots of 1 ml were taken out after different time intervals (0, 4, 6, 8, 12, 24, 48 and 72 h) and ANS and ThT assays were performed. The spectra were corrected by the fluorescence of each probe in the absence of protein and normalized to the recorded maximum intensity of each probe during the misfolding and aggregation reaction.

Single cell gel electrophoresis (SCGE) of the aggregated cyt c

Isolated lymphocytes were exposed to 50 μgm of cyt c aggregates (formed after 72 h) in a total reaction volume of 1.0 ml of 20 mM phosphate buffer pH 7. Incubation was performed at 37 °C for 1 h. After incubation, reaction mixture was centrifuged at 716.8 g, supernatant was discarded, and pelleted lymphocytes were resuspended in 100 μl of PBS and processed further for SCGE. SCGE of aggregated protein was performed under alkaline conditions by the procedure of Khan et al. (2011).

Scanning electron microscopy (SEM analysis)

Aggregates were prepared by taking 10 mg/ml of cyt c in 90 % PEG-400 and 50 % TFE separately and incubating it for 72 h. SEM analysis of the surface and cross-section of

air-dried aliquots of cyt c aggregate was performed with JSM-6510 LV scanning electron microscope (JEOL, Japan). The aliquots were mounted on carbon-tape-coated stainless steel grids operating on an accelerating voltage of 7 kV for PEG-400 and 5 kV for TFE incubated cyt c. Gold plating of the aliquots was done for a clearer image.

X-ray diffraction study

Aggregated cyt c was prepared by taking 2 mg/ml cyt in 90 % PEG-400 and 50 % TFE separately and incubating it for 72 h. After incubation, the protein was air-dried in refrigerator at 4 °C for 24 h to remove solvents, and after that, the samples were poured out on Whatman filter paper so that the remaining moisture gets absorbed there. The studies were carried out using a Rigaku X-ray powder diffractometer with Cu anode (Cu-Kα radiation $\lambda = 1.54186$ Å) in the range of $20° \leq 2\theta \leq 80°$ at 30 kV. Position of the peaks, intensities, widths and shapes all provide important information about the structure of the material.

Results and discussion

Trp fluorescence

Horse cyt c has a single Trp residue at position 59; hence, the most sensitive method of monitoring the gross conformational changes in this protein is to study the Trp fluorescence (Stryer 1968; Amani and Naeem 2013a, b). The fluorescence of PEG-400 and TFE alone was monitored, and here, we report the subtracted fluorescence spectra. Figure 1 summarizes the fluorescence emission spectra of PEG-400 and TFE-induced conformational changes in native cyt c at pH 7. Native cyt c shows quenched fluorescence maximum at 340 nm (curve 1) owing to the close proximity of Trp-59 to heme group. On incubating with 60 % (curve 2) and 90 % (curve 3) PEG-400, cyt c shows a hypsochromic/blue shift of 19 and 15 nm, respectively, accompanied with an enormous increase in fluorescence. On the other hand, cyt c at 40 % TFE (curve 4) showed a blue shift of 10 nm with enhanced fluorescence. This boost may be due to exposure of the Trp residue in the nonpolar environment, suggesting existence of an intermediate state with altered Trp environment. After this, a negligible increase in fluorescence was observed at 50 % TFE (curve 5), indicating saturation in fluorescence. This was accompanied with a red shift of 5 nm relative to intermediate state giving the idea of exposure of Trp residues toward polar environment. Relative Trp fluorescence of cyt c in the presence of PEG-400 up to 20 % concentration showed higher intensity as

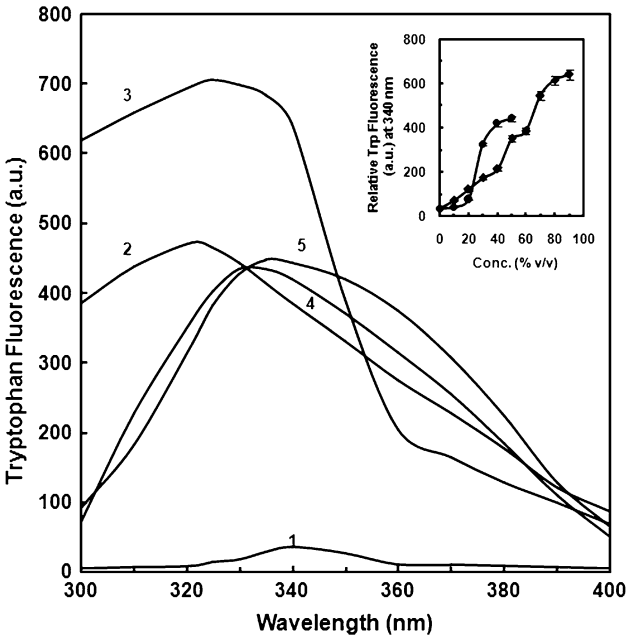

Fig. 1 Trp fluorescence. Emission spectra of cyt c in 20 mM sodium phosphate buffer, pH 7.0 (*curve 1*); in the presence of 60 % (*curve 2*) and 90 % (*curve 3*) PEG-400; in the presence of 40 % (*curve 4*) and 50 % TFE (*curve 5*). *Inset* Relative Trp fluorescence intensity of cyt c as a function of varying concentration of PEG-400 (*filled diamond*) and TFE (*filled circle*). The fluorescence intensity measurement was carried out at an excitation wavelength of 295 nm. Protein concentration was 16.66 μM, and the path length was 1 cm. *Error bars* indicate the mean ± standard deviation ($n = 3$)

compared to TFE. In the presence of TFE, cyt c shows a sigmoidal curve; conversely, in the presence of PEG-400, a bipartite response was observed in fluorescence intensity. Beyond this, a remarkably enhanced Trp fluorescence was observed in the presence of TFE than PEG-400 (Fig. 1, inset). This may be due to ability of TFE to cause extensive protein unfolding relative to PEG-400 at higher concentration. TFE has fluorine group (F^-) which is more electronegative in comparison with OH group present in PEG-400. At lower concentration, the number of OH groups of PEG-400 is more in comparison with F^- of TFE resulting in earlier unfolding. But at higher concentration of TFE, F^- groups impart larger electronegative effect than OH group of PEG-400 masking the number of OH groups, hence resulting in extensive protein unfolding.

Acrylamide quenching

Fluorescence of indole chromophore is highly sensitive to environment, making Trp an ideal choice for reporting protein conformational changes. To rule out the possibility of fluorescence quenching due to Trp residues of cyt c, later were subjected to quenching by uncharged molecules of acrylamide (Caramelo et al. 2003). Figure 2 shows Stern–Volmer plots of free and unbound model compound NATA

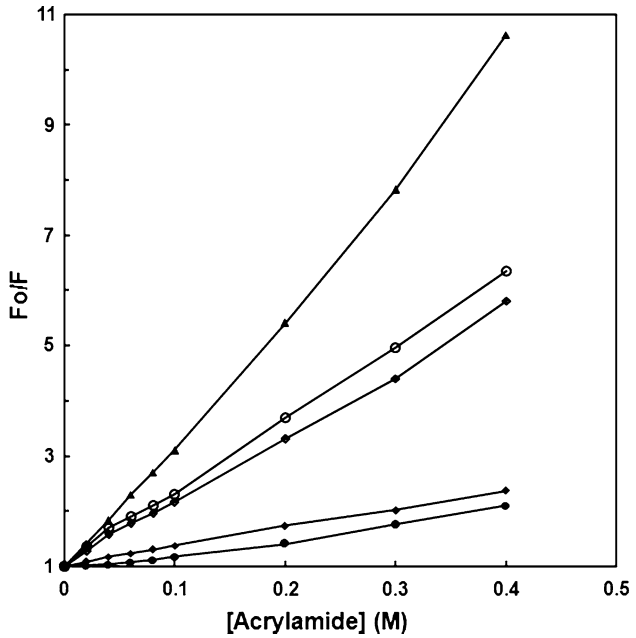

Fig. 2 Stern–Volmer plots for acrylamide quenching of Trp fluorescence of cyt c. Cyt c at 90 % PEG-400 (*open diamond*) and 50 % TFE (*open circle*) and NATA alone (*filled triangle*) after 4-h incubation; cyt c at 90 % PEG-400 (*filled diamond*) and 50 % TFE (*filled circle*) after 72-h incubation. Values shown are the ratios of fluorescence in the absence of acrylamide (F_0) to the fluorescence at that concentration of quencher (F)

and Trp-59 of cyt c in the presence of 90 % PEG-400 and 50 % TFE. The quenching data analyzed from Stern–Volmer plot are shown in Table 1. Quenching experiment on native cyt c showed diminished fluorescence because the close proximity of Trp-59 to heme group results in efficient fluorescence quenching via FRET mechanism. Owing to very weak signals, native cyt c has not been reported. Acrylamide quenching of Trp analog NATA alone shows maximum Stern–Volmer constant (K_{sv}) value indicating maximum quenching. Acrylamide quenching of cyt c (after 4-h incubation) in the presence of 90 % PEG-400 and at 50 % TFE shows shift of λ_{max} from 340 to 332 and 345 nm, respectively. This shift gives an idea about different accessibility of Trp residue to the quencher in the presence of organic solvents. As acrylamide is water soluble quencher and does not penetrate into the hydrophobic core of aggregates, very less acrylamide quenching of cyt c in the presence of PEG-400 and TFE suggests the possibility of aggregation (Naeem and Amani 2013). K_{sv} for acrylamide quenching was found to decrease with aggregation of protein. Larger decrease was observed in TFE-induced aggregates formed after 72-h incubation in comparison with PEG-400, suggesting more potency of TFE to induce aggregation. This decrease may be due to decreased accessibility of Trp to solvent owing to aggregation.

Table 1 Acrylamide-quenching parameters of cyt c in different states

Subjects	K_{sv} (M^{-1})	Incubation time (h)
Cyt c at 90 % PEG-400	13.08	4
Cyt c at 50 % TFE	11.65	4
NATA	24.52	4
Cyt c at 90 % PEG-400	3.369	72
Cyt c at 50 % TFE	2.792	72

The excitation wavelength was 295 nm

ANS fluorescence

Hydrophobic interaction of ANS with protein is one of the extensively used methods for characterizing partially folded state. The fluorescence of PEG-400 and TFE alone was also monitored, and here, we report the subtracted fluorescence spectra. Figure 3 shows ANS fluorescence emission spectra of cyt c at pH 7 in the presence of varying concentration of PEG-400 and TFE. Native cyt c showed negligible ANS binding (curve 1). The maximum ANS emission intensity (~6 times) with a blue shift of 10 nm was observed at 60 % PEG-400 (curve 2). With further increase in concentration of PEG-400 at 90 %, there is a slight decrease in fluorescence intensity of cyt c with a 20-nm blue shift relative to native (curve 3). On the other hand, incubating cyt c with TFE, maximum fluorescence was observed in cyt c at 40 % TFE (~3 times of native) along with a blue shift of 13 nm (curve 4) after that descend takes place till 50 % TFE addition (curve 5). In view of the fact that ANS bind to hydrophobic patches on protein, binding of ANS to hydrophobic regions of cyt c has been used to study the folding intermediates formed during unfolding of this hemeprotein. It can be concluded that at 60 % PEG-400 and 40 % TFE, maximum hydrophobic patches are exposed at cyt c surface resulting in high fluorescence. Similarly, at 90 % PEG-400 and 50 % TFE, the hydrophobic patches of this hemeprotein get buried between the protein molecules causing less ANS fluorescence and thus confirming the formation of aggregates. This state at 90 % PEG-400 and 50 % TFE can be regarded as aggregated state. Comparative to this, TFE shows higher ANS fluorescence than PEG-400 up to 35 % and beyond this, ANS fluorescence diminished until TFE concentration reached 50 % (Fig. 3, inset). However, PEG-400 shows maximum ANS fluorescence at 60 % followed by decline at 70 % with further increase in increase till 90 % addition. Both the solvents showed sigmoidal curve, indicating that lower concentration of TFE causes faster aggregate formation while PEG-400 at higher concentration results in complete aggregation of heme protein.

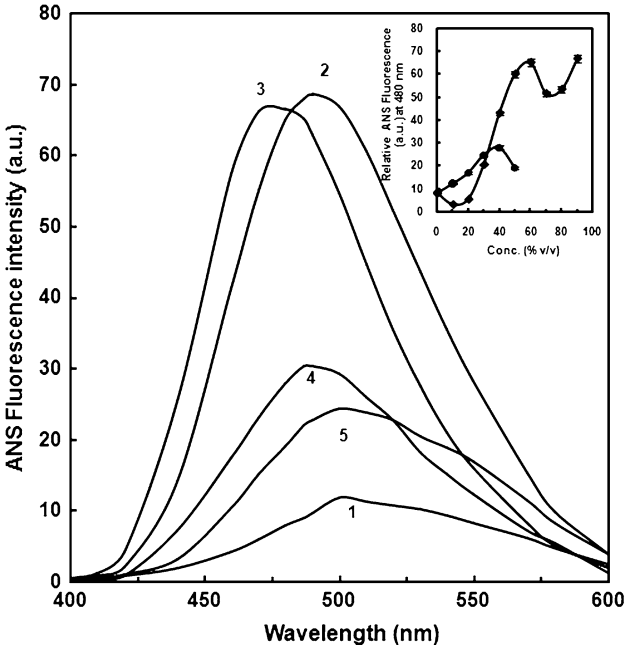

Fig. 3 ANS fluorescence spectra. Emission spectra of native cyt c (*curve 1*); cyt c in the presence of 60 % (*curve 2*) and 90 % (*curve 3*) PEG-400; in the presence of 40 % (*curve 4*) and 50 % TFE (*curve 5*). *Inset* Relative ANS fluorescence intensity of cyt c as a function of varying concentration of PEG-400 (*filled diamond*) and TFE (*filled circle*). The protein concentration was 16.66 μM, and the path length was 1 cm. ANS fluorescence was monitored at an excitation wavelength of 380 nm. *Error bars* indicate the mean ± SD ($n = 3$)

Soret absorbance studies

Soret spectra in cyt c are derived from the interaction between the electronic transitions in the heme and the protein motions in the heme pocket and are sensitive to the environment. Contribution of PEG-400 and TFE alone to the absorption spectra was taken into account, and we report here the subtracted absorption spectra. Heme Fe of native cyt c is axially ligated by two strong field ligands, His18 and Met80, to yield a six coordinated low-spin form. Soret absorption at 410 nm (Fig. 4a) in native cyt c indicates a strong-field low-spin state of the heme iron (curve 1). In the Q-band region (Fig. 4b), a weaker band was observed at 528 nm (curve 1) similar to the results obtained by Wiederkehr et al. (2009). These bands are credited to the transition of the π electrons in the porphyrin. A weak charge transfer band due to electronic transitions at 695 nm is assigned to the S (of Met-80) → Fe ligation (Wilson and Greenwood 1996). In the presence of 60 % PEG-400 (curve 2), the soret band shows a blue shift of 8 nm corresponding to native protein. Blue shift in the soret band indicates that the gap between π and π^* increases in the porphyrin molecule and ultimately resulting in its stabilization (Khare et al. 2006). Also, Q-band splits up into two bands at 520 and 545 nm similar to those observed in reduced cyt c (Mendes et al. 1996). This shift in the Q-band specifies a conformational change mainly in the hydrophobic heme-binding pocket of cyt c. This change is accompanied with disappearance of the peak at 695 nm. These results indicate that the interaction of cyt c at 60 % PEG-400 disrupts Met80-Fe ligation, but still, cyt c is in low-spin state. Perhaps, His33 or His26 instead of Met80 coordinates to heme iron (Khare et al. 2006). In the presence of 90 % PEG-400 (curve 3), soret as well as Q-band shows a blue shift towards 395 and 498 nm, respectively, and a new band emerges at 620 nm, indicating high-spin state of the heme protein. Similarly, in the presence of 40 % TFE (curve 4), 5-nm blue shift in soret band and splitting of Q-band at 522 and 544 nm was observed. At 50 % TFE (curve 5), the conformational changes in the polypeptide are indicated by a blue shift toward 397 and 500 nm, respectively in both the soret and Q-band with the appearance of a new band at 630 nm corresponding to high-spin state of the heme protein (Gong et al. 2003).

Circular dichroism (CD) spectroscopy

Circular dichroism spectroscopy provides information on protein secondary and tertiary structure. The absorption of PEG-400 and TFE alone were taken into account, and here, we report the subtracted spectra. Far-UV CD spectra (Fig. 5a) of native cyt c (curve 1) display minima at 208 and 222 nm, consistent with its known structure in which the 222 nm dichroic band is predominantly associated with α-helical n–π^* amide transitions, and the negative minimum around 208 nm is the dichroic band corresponding to the π–π^* amide transition (Myer 1968). Cyt c at 60 % PEG-400 (curve 2) shows decrease in negative minima corresponding to structural feature of α-helix, signifying its resemblance with native. On further addition of PEG-400, cyt c showed regains negative MRE at 90 % (curve 3), indicating that after an initial drop at 60 %, PEG at higher concentration induces α-helical conformation in cyt c (Arunkumar et al. 1997a). On the other hand, addition of 40 % TFE to native cyt c (curve 4) shows less intense negative minima at 208 and 222 nm suggestive of α-helical structure similar to native. At 50 % TFE (curve 5), cyt c shows minima peaks of α-helical structure, with, the prominent peak at 222 nm and loss of MRE at 208 nm, indicating that this state has more chances to form β-sheet structure on further incubation for longer time period (Arunkumar et al. 1997b). Further, on performing kinetic studies on both of these states, no prominent changes were observed at 24 and 48 h. After 72-h incubation, 90 % PEG-400 induces structural transition from α-helix to β-sheet in cyt c as revealed by a prominent peak at 220 nm (curve 6). Appearance of a new peak at 219 nm in cyt c at 50 % TFE

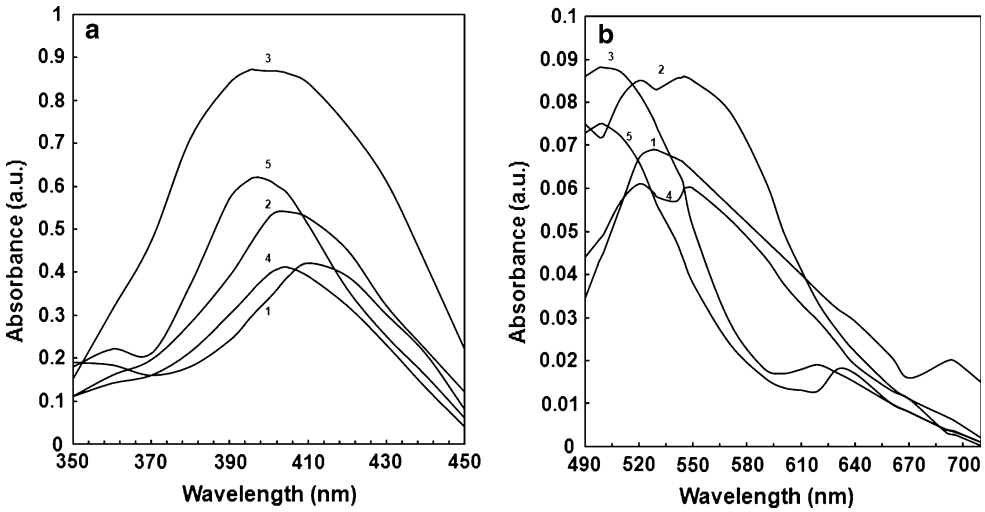

Fig. 4 **a** Soret absorption, **b** Q-band spectra. Cyt c in the presence of increasing concentration of PEG-400 and TFE in sodium phosphate buffer, pH 7.0. Native cyt c (*curve 1*), in the presence of 60 % (*curve 2*) and 90 % (*curve 3*) PEG-400; in the presence of 40 % (*curve 4*) and 50 % TFE (*curve 5*). Cyt c concentration and wavelength range were 16.66 μM and 350–710 nm, respectively. Path length was 1 cm

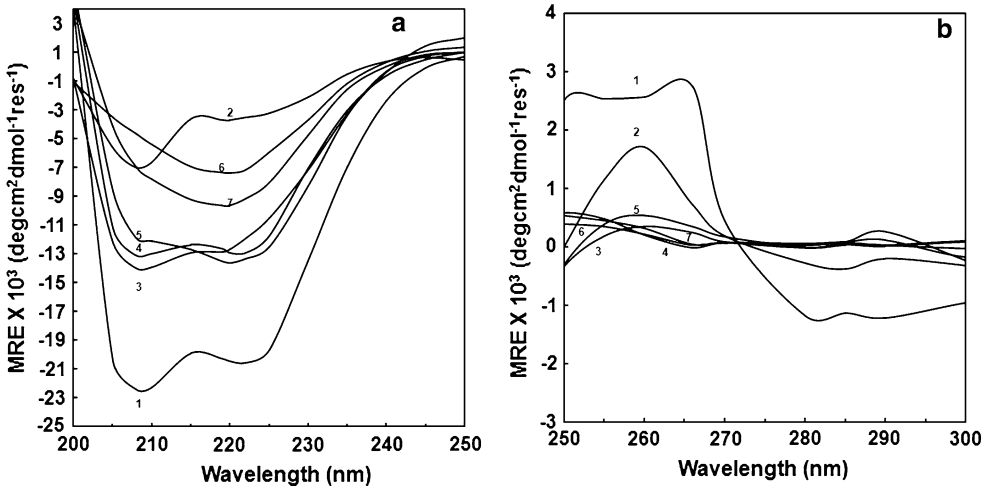

Fig. 5 **a** Far-UV CD spectra. Cyt c in the presence of PEG-400 and TFE in 20 mM sodium phosphate buffer, pH 7.0. *Curve 1* represents native cyt c, cyt c in the presence of 60 % (*curve 2*) and 90 % (*curve 3*) PEG-400; cyt c in the presence of 40 % (*curve 4*) and 50 % TFE (*curve 5*); cyt c at 90 % PEG-400 (*curve 6*) and 50 % TFE (*curve 7*) after 72-h incubation. Cells of path lengths 0.1 cm were used for scanning between 250 and 200 nm, and the protein concentration was 16.66 μM. **b** Near-UV CD spectra. *Curve 1* shows native cyt c, cyt c in the presence of 60 % (*curve 2*) and 90 % (*curve 3*) PEG-400; cyt c in the presence of 40 % (*curve 4*) and 50 % TFE (*curve 5*); cyt c at 90 % PEG-400 (curve 6) and 50 % TFE (*curve 7*) after 72-h incubation. Path length was 1 cm, scanning range was 300–250 nm, and the protein concentration was 40 μM

was observed at the expense of the peak at 208 nm, signifying the presence of β-sheet conformation (curve 7). Reduction in α-helical structure of cyt c caused the partially unfolding of protein, followed by formation of a state with higher β-sheet than α-helical structure contents. β-sheet content was greater in 50 % TFE as compared to 90 % PEG-400.

Near-UV (250-300 nm) CD is a probe for protein tertiary structure changes that affect the environment of aromatic side chains. Horse cyt c contains four phenylalanine residues, four Tyr residues, one Trp and two thio-ether bonds, all of which can potentially contribute to the near-UV CD spectrum. Unfortunately, the interpretation of this region of the CD spectrum is further complicated by the optically active heme transitions that occur between 240 and 300 nm (Urry 1967). Figure 5b shows the near-UV CD spectra of cyt c with varying concentration of PEG-400 and TFE. A broad positive CD band at 250–270 nm and two negative bands between 280 and 290 nm were observed in native cyt c (curve 1). The positive band has been attributed to the transitions in heme (Blauer et al. 1993), whereas negative bands are assigned to the Trp-59 side chain which has been confirmed by their disappearance in a mutant, where Trp-59 is replaced by Phe (Davies et al. 1993). In the presence of 60 % PEG-400 (curve 2), both these negative bands decrease in intensities and the positive band become

more narrow but less intense (~0.5 times) than native, giving maximum intensity around 260 nm. It suggests that state achieved at 60 % PEG-400 has traces of tertiary structure with a native-like secondary structure. These data give an idea that the rigid tertiary structure of cyt c near Trp-59 is practically destroyed at PEG-400 concentration of about 60 %. Some traces of tertiary structure may remain in the neighborhood of the heme leading to its near-UV CD spectrum. At 90 % PEG-400 (curve 3), negative band practically disappears confirming complete structural loss. In TFE-incubated cyt c, intermediate state has been achieved at 40 % TFE (curve 4) showing low-intensity positive band around 250 nm. Further, incubation at 50 % TFE (curve 5) showed occurrence of a state having no prominent intensity. Loss in tertiary structure is because organic solvents disrupt the long-range tertiary contacts of protein native structure and concurrently improve the short-range electrostatic interactions like intermolecular hydrogen bonding by lowering the dielectric constant of the medium. Moreover, incubation of these aggregated states for 72 h, both 90 % PEG-400 (curve 6) and 50 % TFE (curve 7), showed complete loss of negative MRE with a simultaneous increase in positive peak around 290 nm. This indicates that both of these two aggregated state show induction of non-native tertiary structure after 72-h incubation, confirming the formation of aggregates at these concentrations.

Fourier transform infrared spectroscopy (FTIR)

Infrared spectroscopy is one of the oldest and well-established experimental techniques for the analysis of secondary structure of polypeptide and proteins. Figure 6 shows the FTIR spectra of cyt c with varying concentration of PEG-400 and TFE. Cyt c shows a major peak at 1,657 cm^{-1} under native condition (curve 1), confirming its α-helix conformation (Dong et al. 1998). In the presence of 60 % PEG-400(curve 2) and 40 % TFE (curve 4), this peak shifts to 1,651 and 1,653 cm^{-1}, respectively, also ascribed to α-helical conformation. This confirms the retention of α-helical conformation as that of native structure. FTIR spectra of cyt c solution at 90 % PEG-400 (curve 3) show peak at 1,651 cm^{-1}, indicating again, α-helical conformation. This detection was quite different from the widely believed view that β-sheet formation is the general mechanism of aberrant protein aggregation, leading to disease. A similar result has been previously reported in Alzheimer's disease aggregates of Tau protein by Sadqi et al. (2002). On 72-h incubation, cyt c at 90 % PEG-400 (curve 6) shows the emergence of β-sheet-specific peak (1,620 cm^{-1}), signifying the occurrence of conformational transition. Cyt c in the presence of 50 % TFE (curve 5)

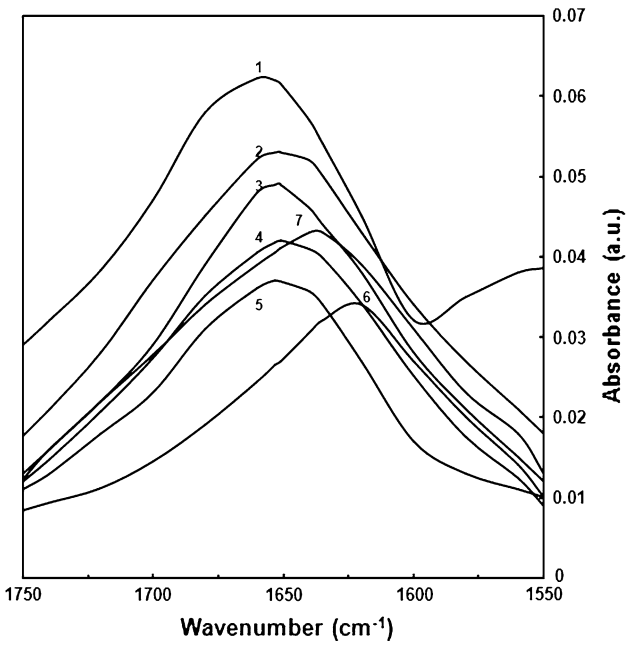

Fig. 6 ATR-FTIR spectra. Spectra in the amide I region of native cyt c (*curve 1*), in the presence of 60 % (*curve 2*) and 90 % (*curve 3*) PEG-400; in the presence of 40 % (*curve 4*) and 50 % TFE (*curve 5*); cyt c at 50 % TFE after 72-h incubation (*curve 6*). Protein concentration was 16.66 μM

shows its maxima peak at 1,653 cm^{-1} which shifts to 1,635 cm^{-1}, on 72-h incubation (curve 7), suggesting a preponderance of β-sheet structure associated by way of *intra*molecular hydrogen bonding, hence confirming α-helix to β-sheet transition. In conformity with CD results, FTIR data showed higher β-sheet content in 50 % TFE-induced aggregates of cyt c compared with 90 % PEG-400 on 72-h incubation. Nelson and Kallenbach (1986) suggested that the weaker dielectric constant of TFE reduces the hydrogen bonding between amide protons and surrounding solvent molecules and promote the intramolecular hydrogen bonding in peptides and therefore stabilizes the secondary structure of peptides. Cammers-Goodwin et al. (1996) suggested that α-helices are most often formed in the presence of TFE because they represent compact conformations that maximize intermolecular hydrogen bonding and minimize solvent exposure. But, with prolonged incubation, cross β-sheets are developed in the molecule due to strong protein–protein interactions, resulting in structural transition from α-helix to β-sheet.

Thus, it can be concluded that at 60 % PEG-400 and 40 % TFE, cyt c exists as molten globule (MG) state with the retention of a compact secondary and traces of tertiary structure, enhanced hydrophobic surface area, altered Trp environment and low-spin state comparable to native.

To further confirm the existence of aggregated states, studies related to fibrillar formation were performed.

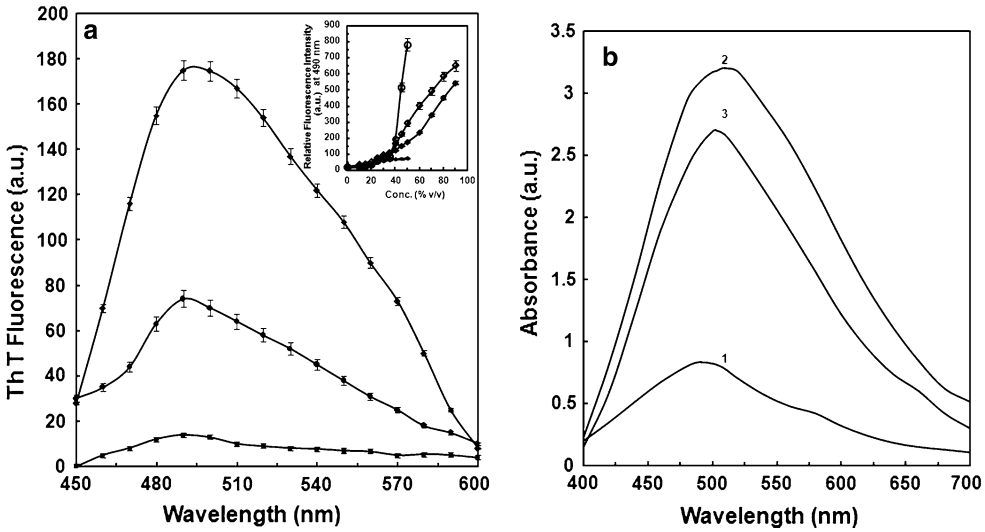

Fig. 7 **a** ThT assay. ThT spectra of cyt c in the presence of 90 % PEG-400 (*filled diamond*); 50 % TFE (*filled circle*) and native cyt c (*filled square*). *Inset* Relative ThT fluorescence of cyt c as a function of varying concentration of PEG-400 (*filled diamond*) and TFE (*filled circle*) incubated for 4 h and PEG-400 (*open diamond*) and TFE (*open circle*) incubated for 72 h. Protein concentration was 16.66 μM, and scanning range was 450–600 nm. *Error bars* indicate the mean ± SD ($n = 3$). **b** Congo red assay. CR absorption spectra of native cyt c (*curve 1*) in 20 mM sodium phosphate buffer, pH 7; in the presence of 90 % PEG-400 (*curve 2*) and 50 % TFE (*curve 3*). The protein concentration was 4 μM. The absorption spectra were recorded from 400 to 700 nm

Thioflavin T assay

ThT molecule consists of a pair of benzothiazole and benzaminic rings freely rotating around a shared C–C bond (Dzwolak and Pecul 2005). ThT behaves as a rotor molecule; it is believed that the increase in quantum yield upon binding results from the inhibition of this free rotation of the rings. The fluorescence of PEG-400 and TFE alone was taken into account, and here, we report the subtracted fluorescence spectra. Figure 7a inset shows the relative ThT fluorescence of cyt c in the presence of varying concentration of PEG-400 and TFE. Maximum intensities were observed in the aliquots having utmost quantity of the organic solvent, that is, 90 % PEG-400 and 50 % TFE. This hike increase in ThT fluorescence indicates the aggregate formation at these concentrations compared to native cyt c. However, 72-h incubation results an abrupt spike in ThT fluorescence after binding with specific β-sheet structure in 90 % PEG-400 and 50 % TFE, confirming the conversion of α-helix to β-sheet structure. A total of 50 % TFE shows higher fluorescence compared with PEG-400, signifying higher β-sheet content in the former case. Also PEG-400, after 4-h incubation at 50 %, shows fluorescence around 12.5 times of the native cyt c (Fig. 7a), and TFE shows maximum fluorescence at similar concentration which is approximately five times of the native. This indicates that PEG-400 has more capacity of inducing aggregate formation in cyt c at 4-h incubation. But, after 72 h, TFE at 50 % shows more fluorescence compared with PEG-400, indicating that with prolonged incubation time, TFE shows enhancement in the capacity of aggregate formation.

Congo red assay

Abnormal protein aggregate associated with various pathologies is commonly detected in tissue with CR. It is also used to monitor amyloid formation in vitro. After ThT, aggregates of cyt c were further confirmed by CR dye as it is more specific and sensitive for amyloid detection. The absorption of PEG-400 and TFE alone was taken into account, and here, we report the subtracted absorption spectra. Native cyt c showed peak at 491 nm (Fig. 7b). In the presence of 90 % PEG-400, a red shift of 19 nm; that is, λ_{max} at 510 nm and at 50 % TFE, red shift of 12 nm accompanied with enhancement in the absorbance was observed; that is, λ_{max} at 503 nm. The interaction between CR and protein is due to the electrostatic interaction between the negatively charged group of CR and positively charged amino acids of protein (Naeem and Amani 2013).

Misfolding and aggregation kinetics monitored by ANS and ThT

Time-course changes accompanying cyt c aggregation were studied to elucidate better fluorescence signals of the probes depending on the conformational state of the protein. This analysis can potentially allow us to discriminate between protein oligomers and larger aggregates. Before

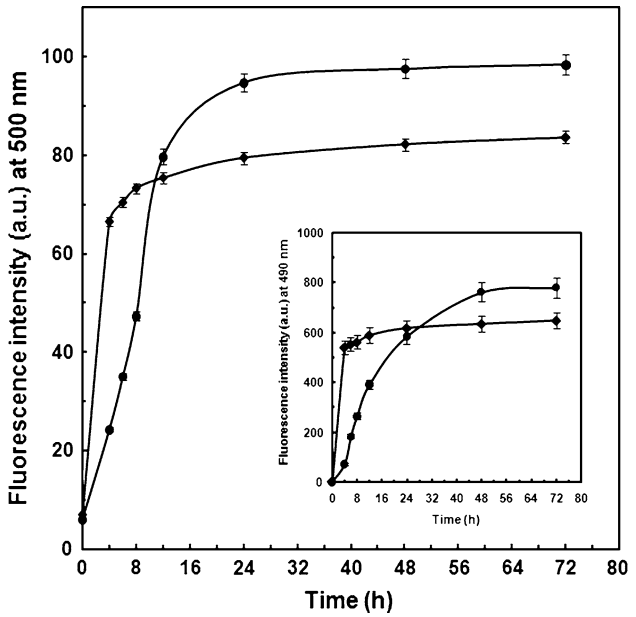

Fig. 8 Aggregation kinetics. Kinetics of cyt c aggregation by PEG-400 (*filled diamond*) and TFE (*filled circle*) followed by ANS and ThT (*inset*). Aliquots of the aggregation reaction were withdrawn and assayed after different time intervals. The concentration of protein in each aliquot was 16.66 μM. *Error bars* indicate the mean ± SD ($n = 3$)

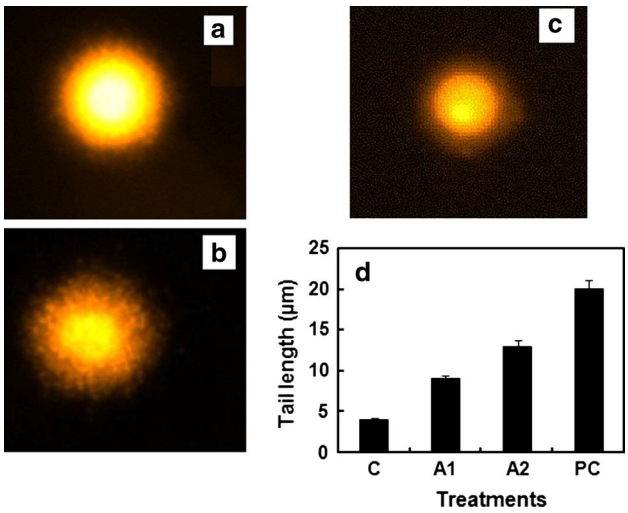

Fig. 9 Single cell gel electrophoresis. Images of lymphocyte nuclei damage **a** in the presence of cyt c at 90 % PEG-400, **b** in the presence of cyt c at 50 % TFE and **c** in the presence of negative control after 72-h incubation, **d** lymphocyte DNA breakage in negative control (NC), treated by cyt c at 90 % PEG-400 (*A1*),cyt c at 50 % TFE (*A2*) and treated by 3 μl of methyl methane sulfonate (25 μg/ml) as positive control (*PC*) after 72 h. Protein concentration was 50 μg. *Error bars* indicate the mean ± SD ($n = 3$). *Significance $p < 0.05$ with respect to *control bar* 'NC'

initiation of the aggregation reaction, cyt c shows almost negligible ANS (Fig. 8) and ThT fluorescence (Fig. 8, inset). The ANS fluorescence of cyt c, in the absence of either PEG-400 or TFE, is minor and is completely silent for ThT. After 4-h incubation, the fluorescence intensity increases approaching maximum at 72 h, suggesting the formation of prefibril and protofibril. ThT showed a very prominent increase in fluorescence in cyt c on 72 h in the presence of TFE and PEG-400, indicating the formation of fibrillar-like structure. TFE induced higher fluorescence compared with PEG-400 signifying the formation of protofibrils in former case compared to later.

SCGE assay

Nuclear DNA damage in lymphocytes by aggregated cyt c in the presence of 90 % PEG-400 and 50 % TFE incubated for 72 h has been shown in Fig. 9a, b, respectively. Negative control (without any treatment) and positive control (3 ml of methyl methane sulfonate (25 mg/ml)) treatments were also performed. Aggregated cyt c caused a significant damage to lymphocytes in vitro, and thus shows its genotoxic potential. Aliquot having aggregated cyt c at 90 % PEG-400 and at 50 % TFE incubated for 72 h added to lymphocytes causes nuclear DNA breakage of about 9 and 13 μm tail lengths, respectively, as compared to 4 μm tail length of negative and 20 μm tail length of positive

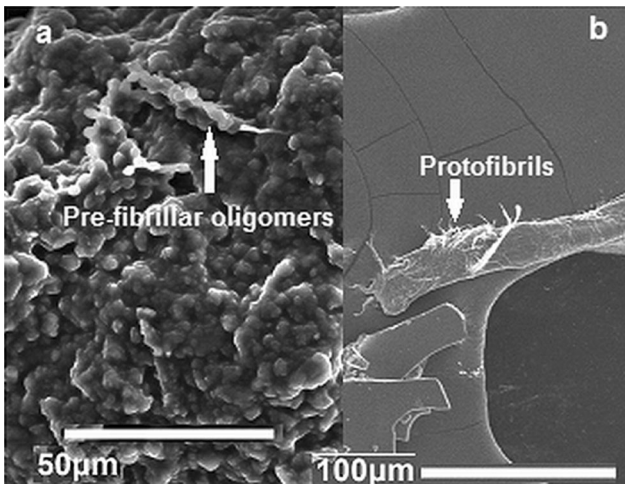

Fig. 10 SEM analysis. Image of cyt c at 90 % PEG-400 (**a**) and 50 % TFE (**b**). Concentration of cyt c was 10 mg/ml

control. Figure 9c depicts the image of negative control (without any treatment) of lymphocytes and bar graph of tail lengths has been shown in Fig. 9d. Damage caused to lymphocyte by aggregated cyt c may be attributed to the fact that the DNA damage is caused by two major mechanisms, free radical reactions and direct binding to DNA. This suggests that apart from oxidative stress to the nucleus, amyloid might bind to the nucleus, thus enhancing

their toxic affect (Jayakumar et al. 2004). As these aggregates are found to be genotoxic to the lymphocytic cells in vivo, this gives us an idea about the damage that they can cause damage to the body cells.

SEM analysis

SEM is used for inspecting topographies of materials with a magnification range that encompasses that of optical microscopy and extends it to the nanoscale. Figure 10a and b shows the SEM images of cyt c at 90 % PEG-400 and 50 % TFE incubated for 72 h separately. Cyt c at 50 % TFE showed the branched morphology resulting in the formation of protofibrils structure. Cyt c at 90 % PEG-400 showed bead-like structure, indicating existence of prefibrillar oligomers.

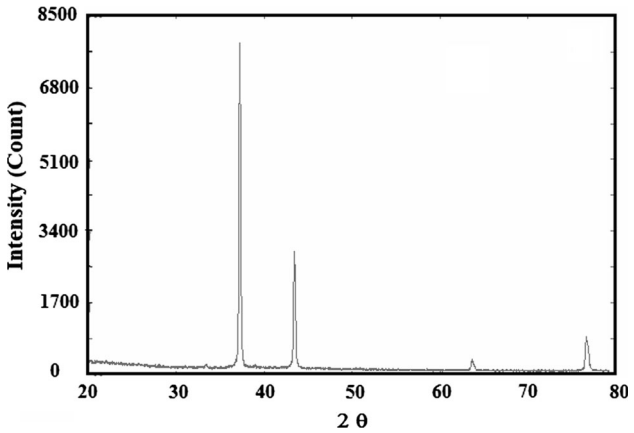

Fig. 11 XRD analysis. XRD analysis of cyt c at 50 % TFE. The X-ray diffraction pattern of cyt c with TFE was recorded at room temperature using a Rigaku Miniflex X-ray diffractometer in 2θ ranging from 20° to 80°. The protein concentration was 2 mg/ml

XRD study

XRD of cyt c at 50 % TFE incubated for 72 h is shown in Fig. 11 as a plot of scattering intensity as a function of scattering angle 2θ. Cyt c at 50 % TFE after 72 h of incubation depicted a prominent peak with high intensity at 2θ of 36° and three small peaks at 42°, 63° and 77° (Fig. 11). Cyt c in the presence of 90 % PEG-400 also exhibited a strong peak around 36° and three small peaks at 2θ of 43°, 64° and 77° with lower intensity than at 50 % TFE (data not shown). However, cyt c in the presence of either 90 % PEG-400 or 50 % TFE showed similar d-spacing value as 4.9 Å, suggesting that in both the cases, fibril formation has started. On the basis of stronger intensity of fibrils in 50 % TFE, they are termed as protofibrils and the other one as prefibrils (Iram and Naeem 2013).

Conclusion

In the present study, MG states of cyt c in the presence of 60 % PEG-400 and 40 % TFE, respectively, (Fig. 12) are analyzed by high ANS fluorescence and retention of secondary structure as revealed by far-UV CD and FTIR

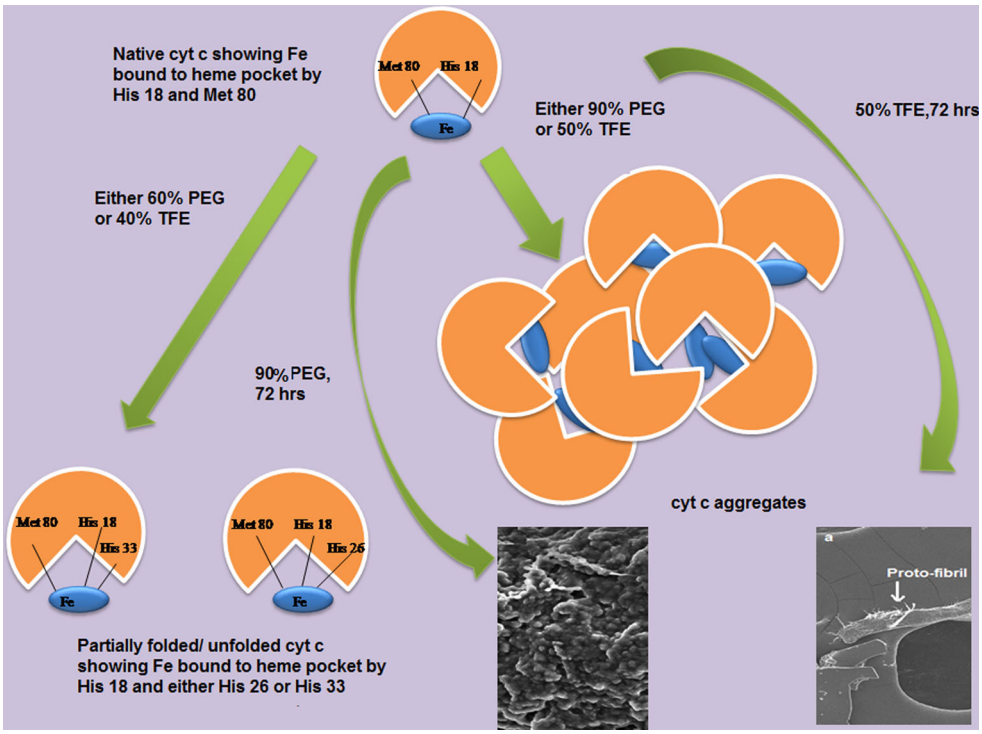

Fig. 12 Overall scheme. Diagrammatic representation of the cyt c transition from native to partially unfolded state, aggregates, prefibrillar oligomers and protofibrils in the presence of varying concentration of PEG-400 and TFE

analysis. A sum of 60 % PEG-400-induced cyt c state showed retention of partial tertiary structure and 40 % TFE-induced cyt c state showed loss in tertiary structure as depicted by near-UV CD. Identification of the structural characteristics of these partially folded states is important for understanding the pathway of protein folding. A total of 72-h incubation of cyt c with increased amount of PEG-400 enhanced ThT fluorescence, and SEM and XRD analysis detected these aggregates as prefibrillar oligomers. TFE at 50 % for 72-h incubation transformed cyt c into the protofibrillar as analyzed by SEM and XRD. Genotoxic potential of these aggregates was confirmed by SCGE and found to possess significant toxicity. Protein misfolding and aggregation is a very common phenomenon in vivo and in vitro conditions and the corresponding biotechnological applications (Naeem and Fazili 2011; Wood et al. 2003). Our work will facilitate a further understanding of the genotoxicity of aggregated protein and conformational changes in the presence of organic solvent and can prove to be very useful in understanding diseases arising due to the formation of aggregates and therapeutical approaches to revert the process of aggregates formation.

Acknowledgments The authors are highly thankful for the facilities available at AMU Aligarh. Authors are thankful to Indo–US Science and Technology Forum for financial support. USIF, AMU has been highly acknowledged for providing SEM facility. S. A. is the recipient of UGC-SRF.

Conflict of interest The authors declare that there are no conflicts of interest.

References

Amani S, Naeem A (2011) Acetonitrile can promote formation of different structural intermediate states on aggregation pathway of immunoglobulin G from human and bovine. Int J Biol Macromol 49:71–78

Amani S, Naeem A (2013a) Understanding protein folding from globular to amyloid state. Aggregation: darker side of protein. Process Biochem 48:1651–1664

Amani S, Naeem A (2013b) Detection and analysis of amorphous aggregates and fibrils of cytochrome c in the presence of phenolic acid. Int J Biol Macromol 58:104–112

Arunkumar AI, Kumar TKS, Yu C (1997a) Non-specific helix-induction in charged homopolypeptides by alcohols. Biochim Biophys Acta 1338:69–76

Arunkumar AI, Kumar TKS, Yu C (1997b) Specificity of helix-induction by 2,2,2-trifluoroethanol in polypeptides. Int J Biol Macromol 21:223–230

Blauer G, Sreerama N, Woody RW (1993) Optical activity of hemoproteins in the Soret region. Circular dichroism of heme undecapeptide of cytochrome c in aqueous solution. Biochemistry 32:6674–6679

Cammers-Goodwin A, Allen TJ, Oslick SL, McClure KF, Lee JH, Kemp DS (1996) Mechanism of stabilization of helical conformations of polypeptide by water containing trifluoroethanol. J Am Chem Soc 118:3082–3090

Caramelo JJ, Castro OA, Alonso LG, De Prat-Gay G, Parodi AJ (2003) UDP-Glc: glycoprotein glucosyltransferase recognizes structured and solvent accessible hydrophobic patches in molten globule-like folding intermediates. Proc Natl Acad Sci USA 100:86–91

Davies AM, Guillemette JG, Smith M, Greenwood C, Thurgood AGP, Mauk AG, Moore GR (1993) Redesign of the interior hydrophobic region of mitochondrial cytochrome c by site directed mutagenesis. Biochemistry 32:5431–5435

Dong A, Matsuura J, Manning MC, Carpenter JF (1998) Intermolecular β-sheet results from trifluoroethanol- induced nonnative α-helical structure in β-sheet predominant proteins: infrared and circular dichroism spectroscopic study. Arch Biochem Biophys 355:275–281

Dzwolak W, Pecul M (2005) Chiral bias of amyloid fibrils revealed by the twisted conformation of thioflavin T: an induced circular dichroism/DFT study. FEBS Lett 579:6601–6603

Eftink MR, Ghiron CA (1982) Fluorescence quenching studies with proteins. Anal Biochem 114:199–227

Eisert R, Felau L, Brown LR (2006) Methods for enhancing the accuracy and reproducibility of Congo red and thioflavin T assays. Anal Biochem 353:144–146

Fiskum G, Starkov A, Polster BM, Chinopoulos C (2003) Mitochondrial mechanisms of neural cell death and neuroprotective interventions in Parkinson's disease. Ann NY Acad Sci 991:111–119

Gong J, Yao P, Duan H, Jiang M, Gu S, Chunyu L (2003) Structural transformation of cytochrome c and apo cytochrome c induced by sulfonated polystyrene. Biomacromolecules 4:1293–1300

Herold DA, Rodeheaver GT, Bellamy WT, Fitton LA, Bruns DE, Edlich RF (1982) Toxicity of topical polyethylene glycol. Toxicol Appl Parmacol 6:329–335

Iram A, Naeem A (2013) Detection and analysis of protofibrils and fibrils of hemoglobin: implications for the pathogenesis and cure of heme loss related maladies. Arch Biochem Biophys 533:69–78

Jayakumar R, Murali J, Koteeswari D, Gomathi K (2004) Cytotoxic and membrane perturbation effects of a novel amyloid forming model peptide poly (Leucine-Glutamic Acid). J Biochem 136:457–462

Khan TA, Amani S, Naeem A (2011) Glycation promotes the formation of genotoxic aggregates in glucose oxidase. Amino Acids 43:1311–1322

Khare N, Eggleston CM, Lovelace DM, Boese SW (2006) Structural and redox properties of mitochondrial cytochrome c co-sorbed with phosphate on hematite (α-Fe_2O_3) surfaces. J Colloid Interface Sci 303:404–414

Kraus A, Groveman BR, Caughey B (2013) Prions and the potential transmissibility of protein misfolding diseases. Annu Rev Microbiol 67:543–564

Margoliash E (1963) Primary structure and evolution of cytochrome c. Proc Natl Acad Sci USA 50:672–679

Mendes SB, Li L, Burke JJ (1996) Broad-band attenuated total reflection spectroscopy of a hydrated protein film on a single mode planar waveguide. Langmuir 12:3374–3376

Myer YP (1968) Conformations of cytochromes. II. Comparative study of circular dichroism spectra, optical rotator dispersion, and absorption spectra of horse heart cytochrome c. J Biol Chem 243:2115–2122

Naeem A, Amani S (2013) Deciphering structural intermediates and genotoxic fibrillar aggregates of albumins: a molecular mechanism underlying for degenerative diseases. PLoS ONE 8:e54061

Naeem A, Fazili NA (2011) Defective protein folding and aggregation as the basis of neurodegenerative diseases: the darker aspect of proteins. Cell Biochem Biophys 61:237–250

Naeem A, Khan RH (2004) Characterization of molten globule state of cytochrome c at alkaline, native and acidic pH induced by butanol and SDS. Int J Biochem Cell Biol 36:2281–2292

Naeem A, Khan TA, Muzaffar M, Ahmad S, Saleemuddin M (2011) A partially folded state of ovalbumin at low pH tends to aggregate. Cell Biochem Biophys 17:271–279

Nelson JW, Kallenbach NR (1986) Stabilization of ribonuclease S peptide by trifluoroethanol. Proteins 1:211–217

Sadqi M, Hernandez F, Pan UM, Perez M, Schaeberle MD, Vila JAA, Munoz V (2002) α-Helix structure in Alzheimer's disease aggregates of tau-protein. Biochemistry 41:7150–7155

Stryer L (1965) The interaction of a naphthalene dye with apomyoglobin and apohemoglobin. A fluorescent probe of non-polar binding sites. J Mol Biol 13:482–495

Stryer L (1968) Fluorescence spectroscopy of protein. Science 162:526–533

Turnell WG, Finch JT (1992) Binding of the dye Congo red to the amyloid protein pig insulin reveals a novel homology amongst amyloid-forming peptide sequences. J Mol Biol 227:1205–1223

Urry DW (1967) The heme chromophore in the ultraviolet. J Biol Chem 242:4441–4448

Wiederkehr WRS, Hoops GC, Aslan MM, Byard CL, Mendes SB (2009) Investigations on the Q and CT bands of cytochrome c submonolayer adsorbed on an alumina surface using broadband spectroscopy with single-mode integrated optical waveguides. J Phys Chem C Nanomater Interfaces 113:8306–8312

Wilson MT, Greenwood C (1996) Cytochrome-c: a multidisciplinary approach. University Science Books, Sausalito

Wood JD, Beaujeux TP, Shaw PJ (2003) Protein aggregation in motor neuron disorder. Neuropathol Appl Neurobiol 29:529–545

Zerovnik E, Skarabot M, Skerget K, Giannini S, Stoka V, Jenko-Kokalj S, Staniforth RA (2007) Amyloid fibril formation by human stefin B: influence of pH and TFE on fibril growth and morphology. Amyloid 14:237–247